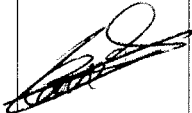

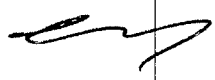


Title

Optical Flow Navigation System For Landing  
—  
Summary Report

	Name & Function	Date	Signature
<b>Prepared by</b>	Cyril CAVEL <i>Studies engineer, advanced studies section</i>	19/03/09	
<b>Verified by</b>	Grégory FLANDIN <i>Head of Automatics, GNC and Formation Flying section</i>	19/03/09	
<b>Approved by</b>	Grégory FLANDIN <i>Optical Flow Study Manager</i>	19/03/09	

Doc type	# WP	Keywords
Technical Note	6.3	GNC, optical flow, soft landing, final report

---

## ABSTRACT

The OFNSL study aims at investigating a promising vision-based landing navigation concept, relying on an optical image processing device and real-time 3D matching functions, for increased robustness and precision, in particular during inclined descent trajectories. This technology offers a valuable alternative to software-based image processing solutions on known landing terrains, while overcoming potential accommodation issues of Lidar-based solutions.

The key challenges raised during this study are:

- the definition of a precision landing navigation solution based on both the optical flow determination from camera images and the matching with a 3D model of the landing site,
- the interface and integration of the optical flow sensor in a vision-based navigation chain,
- the anticipation of a potential real-time demonstration with representative hardware, leading to account for the hardware/software architecture as early as the design phase.

This document is the summary report of the study. It is an output of WP 6.3. This is a synthesis of the main technical findings of the study. The conclusion draws some perspectives for future activities and some recommendations for a future real time experiment on board the PLGTF.

## DOCUMENT CHANGE LOG

<b>Issue #</b>	<b>Date</b>	<b>Modified pages</b>	<b>Observations</b>
1	16/03/2009	All	Creation

---

## REFERENCE DOCUMENTS

- [1] “Application Study for an Optical Correlator”, ESTEC Contract 17572/03/NL/Sfe, Executive Summary.
- [2] “Visual Navigation System for pin-point landing”, ESTEC Contract 18692/04/NL/MU, Summary Report.
- [3] “Functional Model Description of the Optical Flow Chain”, OFNSL study, TUD, 08/2007 (issue 2)

## ACRONYMS


A/D	Analogic to Digital	N/A	Not Applicable
APS	Active-Pixel Sensor	NASA	National Aeronautics and Space Administration
ARP-K	ATV Pre-Development Program Kernel	NPAL	Navigation for Planetary Approach and Landing
AUTONAV	Autonomous Navigation for Interplanetary Missions	OF	Optical Flow
BGA	Ball Grid Array	OFP	Optical Flow Processor
CCD	Charge-Coupled Device	PANGU	Planet and Asteroid scene Generation Utility
CGS	Carlo Gavazzi Space	PLGTF	Precision Landing and GNC Test Facility
CNES	Centre National D'Etudes Spatiales	PM	Progress Meeting
COB	Chip On Board	PRNU	Photo Response Non Uniformity
CPU	Central Processing Unit	RCS	Reaction Control Thruster
CSEM	Centre Suisse d'Electronique et de Microtechnique	RD	Reference Document
DEM	Digital Elevation Map	RMF	Rreference Model-fixed Frame
DSNU	Dark Signal Non Uniformity	S/C	Spacecraft
ECB	Electronic Computing Box	S/W	Software
EDLS	Entry Descent and Landing System	SCIS	Spectrum Correlation Image Sensor
EKF	Extended Kalman Filter	SLAM	Simultaneous Localization And Mapping
ESA	European Space Agency	SLM	Spatial Light Modulator
FEIC	Feature Extraction Integrated Circuit	SNR	Signal to Noise Ratio
FOV	Field Of View	SOW	Statement of Work
FPGA	Flexible Programmable Gate Array	TBD	To Be Defined
GNC	Guidance Navigation and Control	TCP/IP	Transmission Control Protocol/Internet Protocol
GSTP	General Support Technology Program	TCT	Transverse Control Thruster
HINAV	Robust Multi-Mission Hybrid Navigator Breadboard	TM/TC	TeleMeasure / Telecommand
I/F	Interface	TMS	Thruster Management System
ICIU	Inertial & Computer Integrated Unit	TOF	Time Of Flight
IGT	Image Generation Tool	TRP	Technological Research Programme
IMU	Inertial Measurement Unit	TRR	Test Readiness Review
IP	Image Processing	TUD	Technische Universität Dresden
ITT	Invitation To Tender	VBNAT	Vision Based Navigation Analysis Tool
IVN	Integrated Vision and Navigation for Planetary Exploration	VBNC	Vision Based Navigation Camera
JTC	Joint Transform Correlation	VBRNAV	Vision-based Relative Navigation
JTOC	Joint Transform Optical Correlator	w.r.t.	with respect to
KDE	Kinematics, Dynamics and Environment	WP	Work Package
LDS	Landing Site Frame		
LIDAR	Laser Imaging Detection and Ranging		
LiGNC	Lidar Based GNC for Rendezvous and Landing		
LOS	Line of Sight		
MET	Main Engine Thruster		
MSL	Mars Science Laboratory		
MTF	Modulation Transfer Function		

## TABLE OF CONTENTS

<b>1</b>	<b>GENERAL INTRODUCTION</b> .....	<b>8</b>
<b>2</b>	<b>MISSIONS REVIEW AND REFERENCE SCENARIOS</b> .....	<b>9</b>
2.1	MOON LANDING APPLICATION .....	9
2.2	MARS LANDING APPLICATION .....	10
2.3	ASTEROID LANDING APPLICATION .....	12
2.4	SELECTION OF BASELINE MISSIONS.....	12
<b>3</b>	<b>NAVIGATION SYSTEM REQUIREMENTS</b> .....	<b>13</b>
<b>4</b>	<b>NAVIGATION DESIGN</b> .....	<b>15</b>
4.1	MAIN DRIVERS .....	15
4.1.1	<i>Ensuring the robustness of the system</i> .....	15
4.1.2	<i>Avoiding algebraic loops between measurements and aidings</i> .....	16
4.1.3	<i>Tuning the frame rate to improve system performances</i> .....	16
4.2	NAVIGATION ARCHITECTURE AND INTERFACES.....	17
<b>5</b>	<b>NAVIGATION PERFORMANCES</b> .....	<b>20</b>
5.1	OPEN LOOP TESTS .....	20
5.1.1	<i>Test plan</i> .....	20
5.1.2	<i>Test results (OF navigation solution / Moon Mission)</i> .....	22
5.1.3	<i>Test Results (VOF Navigation solution / Mars Mission)</i> .....	24
5.1.4	<i>Conclusion of the open loop tests</i> .....	26
5.2	CLOSED LOOP TESTS.....	26
5.2.1	<i>Simulator integration</i> .....	26
5.2.2	<i>Objectives of the closed loop simulations and test plan</i> .....	27
5.2.3	<i>Tests results</i> .....	27
5.2.4	<i>Conclusions of the closed loop tests</i> .....	31
<b>6</b>	<b>CONCLUSION AND PERSPECTIVES</b> .....	<b>32</b>
6.1	AN INNOVATIVE VISION-BASED NAVIGATION TECHNOLOGY FOR LANDING.....	32
6.2	PRELIMINARY DEVELOPMENT PLAN FOR A FLIGHT EXPERIMENT.....	33

## TABLE OF FIGURES

Figure 2-1 : Reference trajectory for Moon .....	10
Figure 2-2 : Reference trajectory for Mars .....	12
Figure 4-1 : Top-level navigation architecture.....	18
Figure 5-1 : Navigation errors dependency on the minimal sampling time limit (averaged for 5 ... 30 s mission time).....	22
Figure 5-2 : Navigation errors (RSS for 3 axes) obtained with different values of initial estimation errors scaling coefficient.....	23
Figure 5-3 : Navigation errors dependencies on the sampling interval value.....	24
Figure 5-4 : Navigation errors (RSS for 3 axes) obtained with different values of initial estimation errors scaling coefficient.....	25
Figure 5-5 : Moon scenario - True position and velocity in LDS.....	28
Figure 5-6 : Moon scenario - Estimation errors.....	29
Figure 5-7 : Mars scenario – true position and velocity in LDS .....	30
Figure 5-8 : Mars scenario – Estimation errors.....	31
Figure 6-1 : PLGTF and OPTICAL FLOW equipment .....	34

	<b>Optical Flow Navigation System for Landing</b>	Ref : <b>OPTICAL.ASTR.TN.003.09</b> Issue : 1      Rev. : 0 Date : 16/03/2009 Page : 8
---	---	---

## 1 GENERAL INTRODUCTION

The concept to be evaluated in the OFNSL study, namely the Optical Flow Navigation, is complementary to the feature point tracking approach developed in the NPAL study, and is part of the same technique family, i.e. the Vision Based Navigation. This innovative navigation concept is based on an optical implementation of the image processing of the approached planet surface images and the matching of 3D surface models of the landing site.

This study corresponds to the continuation of two ESA studies, namely the *Application Study for an Optical Correlator* and the *Visual Navigation System for Pin-Point Landing* study, both performed by TU Dresden and Astrium ([1] and [2]). The objective of the OFNSL study is to push the concept further, from open and closed loop simulations to the feasibility of an embedded experiment.

To obtain the required accuracy and reliability of navigation data determination, the idea is to match not only the 2D images, but 3D reference model of the planet surface, stored on board. Current 3D models of the approaching surface will be produced by real time processing of the images sequence from the onboard navigation camera. First, for each pair of sequential images, the optical flow is determined, which corresponds to the vector field, characterizing the image motion pattern from frame to frame. The Optical flow field contains the translational component, caused by translational motion of the camera, and rotational component, caused by camera rotation (change of attitude). Only the translational component contains the information about the 3D environment. Using the determination of the camera attitude change, coming from IMU, the rotation component is removed before extraction of the 3D information.

The optical flow matrix is then converted into the 3D model of approaching surface, in a form of Digital Elevation Model (DEM). Currently obtained 3D surface models are matched with the reference model (obtained from the orbital observations). The matching is understood as finding the geometrical transformation, which aligns the obtained and reference surfaces. Matching is performed by multi-point correlation of the fragments of both DEM, treated as the 2D images with the local height represented by brightness. As for other vision-based navigation concepts, the velocity cannot be recovered independently from the distance to the plane. This is solved by using the camera estimated position/attitude aidings coming from the Navigation filter for the matching process as a first guess in an iterative process.

To achieve the real time performance, both optical flow determination and 3D models matching will be done using the onboard optical correlator – optoelectronic device, capable of extremely fast image processing due to application of high parallel optical computing.

Matching of 3D models instead of 2D images is not sensitive to the perspective distortions (but the in-orbit generation of the reference DEM is) and is therefore suitable for inclined descent trajectories. It is also not affected by illumination variations. The redundancy of matching the whole surface instead of the individual reference points ensures high reliability of matching and high accuracy of obtained navigation data, i.e. position and attitude, to be provided to the Navigation filter, for hybridization with the IMU. Conversely, aidings coming from the IMU may help refine the correlation, predict the motion, compensate the distortion...

This technology can be of high interest when absolute positioning with respect to the surface is needed.



## 2 MISSIONS REVIEW AND REFERENCE SCENARIOS

This chapter is dedicated to a review of potential missions applicable to the Optical Flow Navigation System for Landing study. As stated in the SOW, and in accordance with the AURORA program, the study focuses on robotic missions to Moon, Mars and asteroids.

The aim of the AURORA programme is to define and implement an approach that Europe would follow to explore the Planets of the Solar System, with a special emphasis on the Moon, the asteroids and Mars, the goal of this programme being ultimately a Human Mission on the red planet. AURORA can be seen as road map for science and human exploration, from which a number of scientific returns as well as technology spin-offs will emerge. In 2001, ESA (supported by the European industry) proposed a preliminary road map for missions with what can be considered, at the current time, as a realistic goal in terms of planned funding, technology achievements and programmatic. This Plan was foreseeing an approach in 3 phases:

- First phase: in-situ exploration with exobiology packages, in-situ characterization of the planet looking for signs of past or present life with ExoMars mission, and Mars sample return missions;
- Second phase: extensive planetary analysis by robotics means, up to a permanent robotic presence on the surface of Mars;
- Third phase: set-up of the Martian infrastructure for the first Human Mission.

### 2.1 MOON LANDING APPLICATION

Under ESA contract, Astrium SAS has proposed a lunar mission providing demonstration for autonomous rendezvous and for soft & precise landing technologies: the MoonTwins mission, for Moon Technological Walk-through and In-situ Network Science. This mission is also offering an innovative and valuable geosciences network capability.

The MoonTwins mission proposed by Astrium would allow answering within 10 years the most pressing scientific questions and providing precious information in support of a manned-colony.

The MoonTwins baseline mission concept, as a MSR precursor mission, is to send two landers in orbit around the Moon, to use them to experiment as much as possible the rendezvous technologies and operations required by MSR, and to land them near the lunar South and North poles.

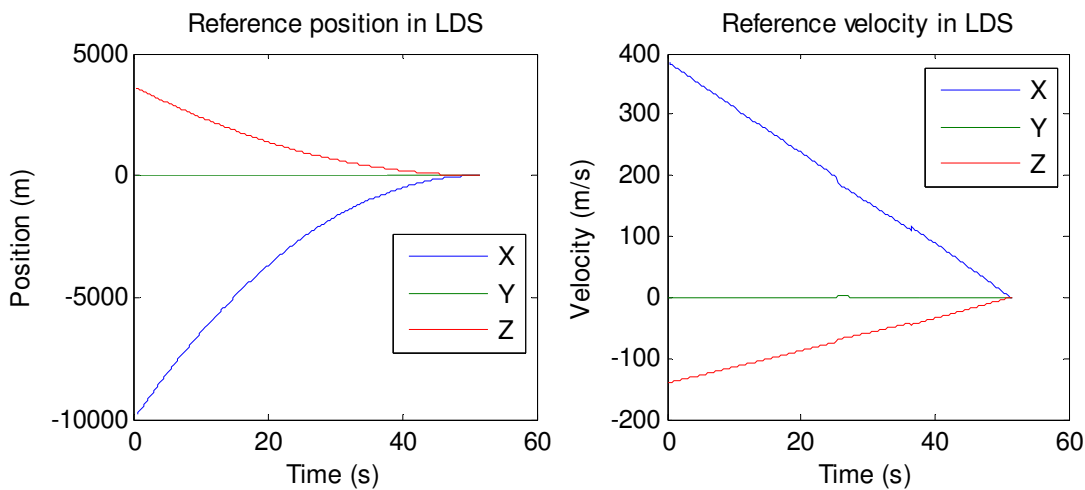
The landing phase shall demonstrate that Europe masters the soft precision landing GNC technologies including hazard avoidance, thus preparing ESA optimally for a fruitful cooperation with NASA on MSR. Furthermore a short ascent phase experiment shall tentatively be conducted just after landing. The science return of the mission shall primarily consist in a seismometer network with two surface packages diametrically opposed, providing the best possible characterisation of the Moon interior. Furthermore two additional Moon geosciences payloads, a Laser transponder and a heat flux mole, shall be considered to

complement the science, but this will be subject to optimisation during the study according to ESA science priorities.

Last but not least, the mission shall achieve a major step forward in the ESA Aurora exploration initiative, by being potentially the first ever Moon lander to reach the Peak of Eternal Light near the rim of crater Shackleton at the South Pole, where NASA and other space agencies intend to place the future manned lunar base. This achievement and the environmental science that can be performed at this famous location will provide unique and high value assets to ESA for future international exploration initiatives, as well as a major Public Relation impact.

Another mission to Moon which would be relevant for the Optical Flow study is the LES 3 mission (European Robotic Lunar Mission), conducted by ESA. The objectives of LES 3 are to provide a European technology demonstration platform for specific technologies needed for Lunar and Mars exploration and to provide a scientific payload platform for specific measurements needed for future Lunar explorations.

The lunar reference trajectory chosen for the OFNSL study is an inclined descent with a slope of 20 deg. The trajectory lasts about 50 seconds and is represented in Figure 2-1, in the terrain frame (LDS).



**Figure 2-1 : Reference trajectory for Moon**

## 2.2 MARS LANDING APPLICATION

Two automatic missions to Mars were recently studied by Astrium, in the frame of proposals in response to ESA Invitations to Tender: ExoMars and Mars Sample Return.

The lander of ExoMars is much lighter than MSR's lander, which authorises a landing with airbags, instead of a soft landing. It relaxes the constraints on landing safety, since airbags are a simple protection against terrain hazards. The field of application of the Optical Flow study being the soft landings (i.e.

landings at low speed on legs), the MSR mission is therefore naturally the most relevant reference for this study. We have therefore defined a reference scenario that is mostly based on the MSR scenario.

The specifications for Martian scenarios are the following:

- a. the trajectory type corresponds to "gravity turn" strategy
- b. the descent duration is around 60 s
- c. initial velocity should be in the range of 70 to 100 m/sec
- d. initial altitude is around 2000 m
- e. maximum angular rate is 10 deg/s

Several scenarios could also be evaluated:

- f. test attitude oscillations due to descent under parachute
- g. perturbations due to atmosphere : constant wind, wind gusts

No retargeting manoeuvre is planned as the landing site is pre-defined using the reference DEM.

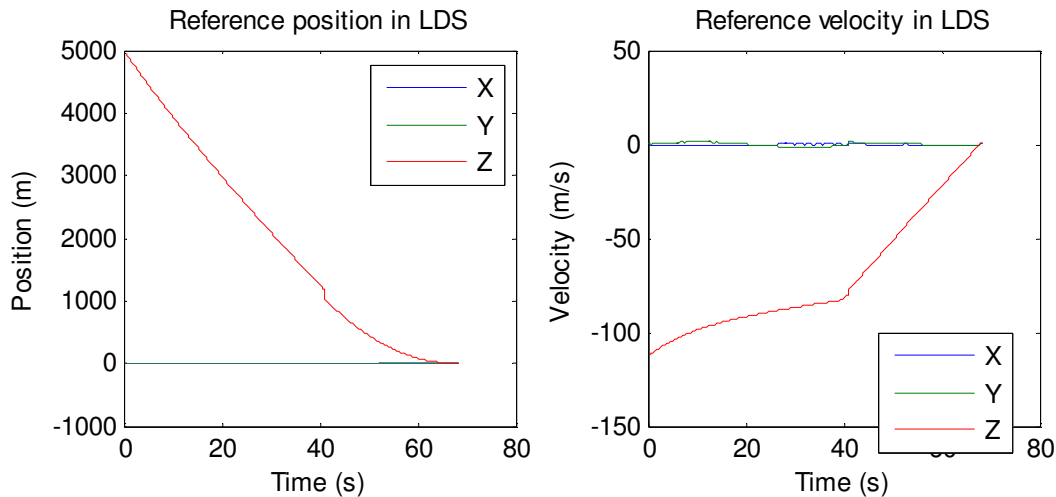
The Descent Module (DM) will approach Mars on a dedicated carrier spacecraft, upon arrival the DM will approach the planet on a hyperbolic trajectory that will bring it into the upper atmosphere. Initial braking will be provided by the front shield of the aeroshell. At Mach 2.0 and an altitude of approximately 7.6km, a drogue chute will be deployed to stabilise the DM through the transonic regime and reduce its velocity to Mach 0.8. The Back cover of the DM will then be released with the drogue chute and a main parachute will be deployed to reduce the velocity further. Once the terminal velocity of the parachute is reached at an altitude of about 3.5km (or 1.5km above the 2km maximum altitude landing site) the parachute is released and the remaining descent is performed using chemical propulsion before finally touching down with a velocity of  $\leq 2$ m/s.

The Mars descent scenario is divided into 3 different phases in terms of dynamics:

- **Phase 1** : 40 s duration under parachute, starting from initial altitude  $h_0 = 5200$  m, initial velocity  $V_0 = 110$  m/s and initial angle with respect to vertical of 15 deg, which induces swing motion. This phase ends after 40 s, which corresponds to the parachute jettisoning at an altitude of 1500 m and with a velocity of 80 m/s.
- **Phase 2** : 32 seconds duration, with a Main Engine thrust of 1800N. Final Altitude at MECO is 40m and final Velocity is 2.5m/s.

- **Phase 3** : final descent with main engine off, the RCS thrusters continue to break the lander down to the ground. Final velocity shall be compatible with a landing using legs (1 m/s).

Figure 2-2 plots the reference trajectory in the LDS frame (terrain frame, Z is vertical).



**Figure 2-2 : Reference trajectory for Mars**

### 2.3 ASTEROID LANDING APPLICATION

The NEA study (Near Earth Asteroids) that has been conducted by Astrium under ESA contract is relevant for using the optical flow technique for soft and precise landing. The Marco Polo mission (which is built upon NEA technical heritage) is a good candidate for Cosmic Vision 2015-2025.

The purpose of this mission is to make a sample return. The landing shall be performed at a pre-defined site with high accuracy to avoid hazards, which makes the optical flow technique quite interesting for this mission.

The asteroid scenario has not been simulated during the OFNSL study as no trajectory is available at this stage.

### 2.4 SELECTION OF BASELINE MISSIONS

In conclusion, the baseline missions are the following:

- ✓ Moon mission : Moon Twins
- ✓ Mars mission : MSR
- ✓ Asteroid mission : Marco Polo

### 3 NAVIGATION SYSTEM REQUIREMENTS

The requirements given in the Statement of Works specify the performance of the Navigation estimation for position and velocity, respectively 10 m and 1 m/s. The performance of the navigation estimation for the attitude shall be better than 1 deg. These values are  $3\sigma$  figures and are specified for the touchdown.

Regarding the requirements in terms of position and velocity determination, the concepts of absolute and relative Navigation requirements shall be defined. Absolute Navigation requirements are defined with respect to some fixed reference relative to the celestial body, which could be a site of high scientific interest, or a designated site resulting from a preliminary analysis of the potential landing areas.

Relative navigation requirements are defined with respect to the approached ground. Essentially, the relative navigation principle consists in processing evolving measurements, coming for example from the navigation camera. The resulting information is combined with an inertial navigation, which provides the movement between successive images.

Requirements are also specified in terms of robustness to external perturbations such as the lightning conditions, which can be very different between Moon scenario and Mars scenario, jitter or smearing effects. Another important aspect of the requirements concerns the optimization of the resources required by the Navigation Algorithms, in terms of memory allocation and computing time. The Navigation filter and the associated processing functions should be compatible with real-time constraints for the use in the future experiment platform.

The objective of the study is to design a Moon and Martian landing system that guarantees a safe and accurate landing on ground. The landing site can be precisely designated on the basis of previous observation missions, or only approximately characterized before that the landing occurs.

This objective of safe landing can be further detailed by the following high-level specification for the GN&C system:


1. The GN&C design shall guarantee at extinction of main thrusters that the range and transverse **velocities are controlled with an accuracy better than 10 cm/s.**
2. The GN&C design shall be compatible with **legs as landing gear.** In particular, velocity at touchdown shall be lower than 1 m/s.
3. The **kinematics/attitude conditions** at Touchdown shall guarantee a safe landing.
4. For Mars Scenario, the GN&C shall be compatible with steady wind up to 20 m/s (horizontal velocity) and wind gusts up to 15 m/s. The GN&C shall also be compatible with the presence of dust.
5. The GN&C shall be able to land on **terrain with high scientific interests**, which might present **unfavourable slope (up to 20 deg) and roughness statistics (the percentage of area covered with rock higher than 1.5 m is less than 10 %).**

6. After landing and immobilization, the **lander attitude** shall be less than 2 deg with respect to local vertical.
7. The **maximum over-consumption**, which is a system-level requirement, should be less than 5% of the final mass.
8. The GN&C design shall be robust to varying **illumination conditions**.

The table below summarizes the reference mission selected for each application case along with their main characteristics about environment, landing site location and trajectory. The main navigation requirements are synthesized in this table. Position and velocity requirements are relative to the ground.

	Moon	Mars	Asteroids
Reference mission	Moon Twins	MSR	NEA
Main ground characteristics	<ul style="list-style-type: none"> <li>. No atmosphere</li> <li>. Heavily cratered</li> <li>. LS at poles</li> </ul>	<ul style="list-style-type: none"> <li>. Atmosphere : wind, dust</li> <li>. Smoother terrain</li> <li>. LS in 5-15 deg S</li> </ul>	<ul style="list-style-type: none"> <li>. Fewer information</li> <li>. heavily cratered</li> </ul>
Trajectory for VGP	<ul style="list-style-type: none"> <li>. Oblique descent (20 deg)</li> <li>. 600 m/s, 6 km, 100s</li> </ul>	<ul style="list-style-type: none"> <li>. Gravity turn : vertical descent</li> <li>. 70 m/s, 2 km, 60s</li> </ul>	<ul style="list-style-type: none"> <li>. Quasi vertical descent</li> <li>. Hovering at a gate position</li> <li>. Contamination issue</li> </ul>
Nav. Requirements (touchdown, $3\sigma$ )	<ul style="list-style-type: none"> <li>. Velocity estimation accuracy : 1 m/s</li> <li>. Position estimation accuracy : 10 m</li> <li>. Attitude estimation accuracy : 1 deg</li> </ul>		

**Table 3-1 : Synthesis of reference mission, characteristics and navigation requirements**

	<b>Optical Flow Navigation System for Landing</b>	Ref : <b>OPTICAL.ASTR.TN.003.09</b> Issue : 1      Rev. : 0 Date : 16/03/2009 Page : 15
---	---	--

## 4 NAVIGATION DESIGN

### 4.1 MAIN DRIVERS

This chapter details the main drivers that have been considered to design the navigation architecture, and the interfaces between the navigation core and the optical correlator.

#### 4.1.1 Ensuring the robustness of the system

The optical correlator chain is composed of two main stages, as presented by University of Dresden (see RD [3]):


- ✓ The first stage is the egomotion function: based on images correlation, it determines the optical flow observed between the two images and uses this information to deliver a first set of measurements to the navigation filter.
- ✓ The second stage of the optical flow chain is the DEM matching function, which generates and matches the OF-derived DEM with the reference DEM to deliver a second set of measurements to the navigation filter.

To ensure a good robustness to the system, these two functions shall remain independent one to the other as much as possible. The objective is to ensure that if the DEM matching function is not operational for any reason, the egomotion function keeps delivering its measurement to the navigation filter.

This has a twofold impact:

- ✓ The nature of the measurements provided by each of the stages of the optical flow chain shall be defined in order to ensure that the first measurement can be independent of the second one,
- ✓ Feedback interfaces between the two stages shall be avoided as much as possible.

Using a correlation of two images, the egomotion function is able to observe the translation direction and the attitude change between the two images through the optical flow. It is not straightforward to discriminate the part of the optical flow that comes from the translation to the part coming from the rotation. Therefore, it is preferable to consider that the egomotion function gets the knowledge of the attitude change thanks to IMU measurements integration between the two images, so as to ease the determination of the translation direction. The single measurement provided by the egomotion function to the navigation filter will then be the translation direction between the two images.

	<b>Optical Flow Navigation System for Landing</b>	Ref : <b>OPTICAL.ASTR.TN.003.09</b> Issue : 1      Rev. : 0 Date : 16/03/2009 Page : 16
---	---	--

The second stage of the optical flow chain is able to measure the relative position of the lander to the ground and its attitude, using the DEM matching. For the same reason, only the relative position of the lander will be computed by this function and provided to the navigation filter. IMU data will be used to get the knowledge of the attitude change.

With this measurement definition, no feedback from the DEM matching function to the egomotion function is required, ensuring the robustness of the system

#### 4.1.2 Avoiding algebraic loops between measurements and aidings

During the past vision-based navigation studies led by Astrium, it appeared that algebraic loops between sensor's measurements and the navigation filter must be avoided as much as possible. Such loops can occur through aidings provided to the sensor by the navigation filter if the sensor uses directly this aiding as part of the final measurement. This can lead to instability problems.


As written in the previous section, egomotion and DEM matching functions require knowing the attitude change between the two images. It is much preferable that this data comes from the IMU instead of the navigation filter itself. A dedicated function is therefore required to compute the required aiding by processing IMU measurements.

#### 4.1.3 Tuning the frame rate to improve system performances

The egomotion function computes the optical flow between two frames in order to determine the vanishing point in the image to get the translation direction. The frame rate has a direct impact on the performance of the translation direction determination: if this frame rate is high, then the distance covered between the two frames will be small and the signal-to-noise ratio will be degraded. It is then preferable to decrease the frame rate to ensure a correct  $dz/z$  ratio. According to the experience of University of Dresden, this ratio shall be kept around 10% during the descent (see RD [3]). Considering the dynamics of the trajectory, this means that the frame rate can not be constant and shall be computed in real-time to ensure this 10% ratio.

The main impact on the navigation architecture is the need of a dedicated function that selects the pairs of images to be used by the optical correlator. This function will be performed by the optical correlator itself. No navigation data is required.



	<b>Optical Flow Navigation System for Landing</b>	Ref : <b>OPTICAL.ASTR.TN.003.09</b> Issue : 1      Rev. : 0 Date : 16/03/2009 Page : 17
---	---	--

## 4.2 NAVIGATION ARCHITECTURE AND INTERFACES

This section presents the navigation architecture that has been defined considering the main constraints expressed in the previous section.

Figure 4-1 schemes the top-level navigation architecture. It is made of three main components:

- ✓ Sensors: they are the NPAL camera and the Inertial Measurement Unit,
- ✓ Optical Flow algorithms: the optical flow chain has been divided in two main functions as explained before. The first one is the OF & egomotion function, the second one is the DEM matching function. A third block is the IMU increments pre-processing function, which computes the aidings required by the two OF functions (delta position and attitude between the two frames).
- ✓ Navigation Core: this is the navigation filter and the aidings computation function.

One can see that there is no feedback from the DEM matching function to the OF & egomotion function, for the reasons explained in the previous section.

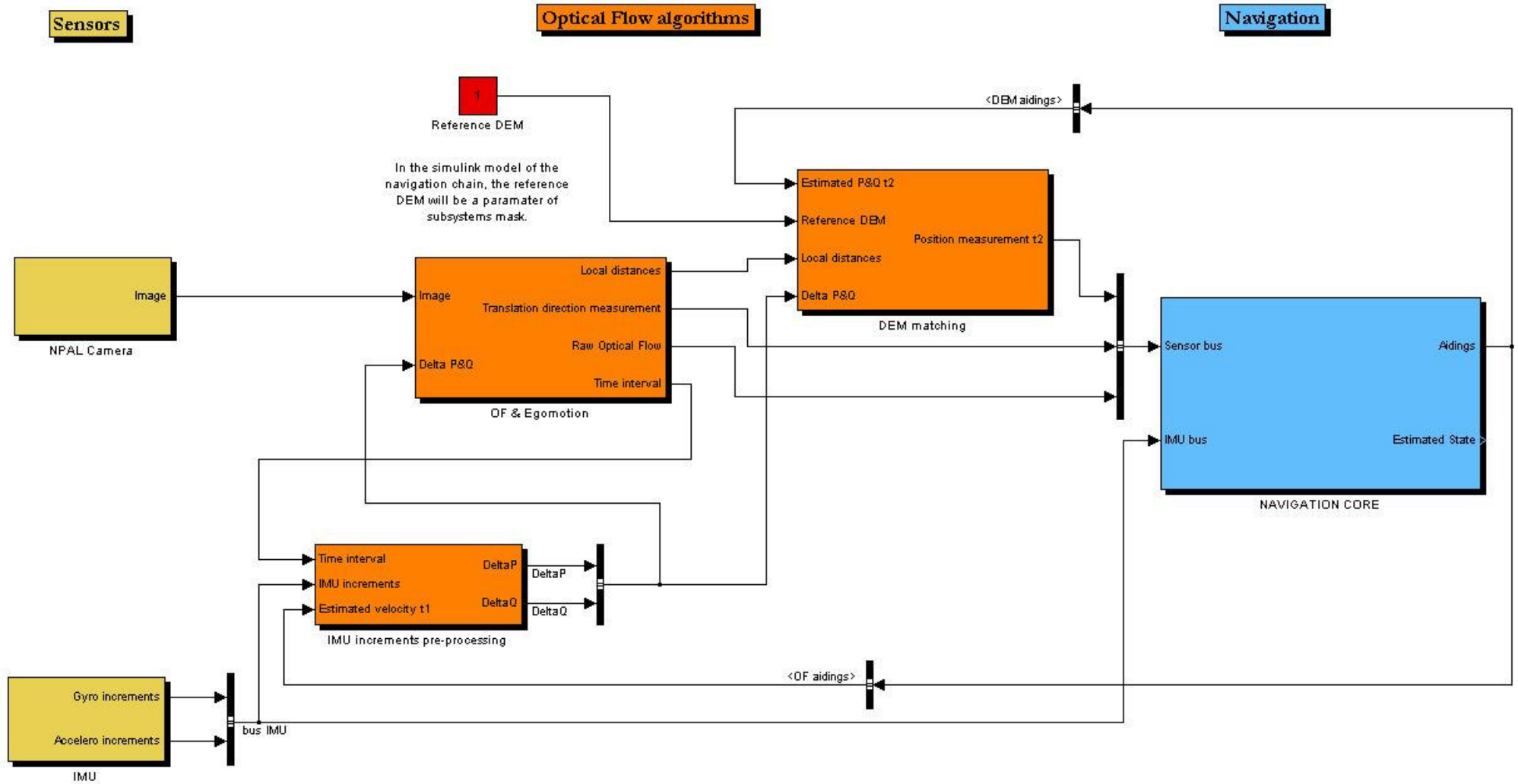



Figure 4-1 : Top-level navigation architecture

	<b>Optical Flow Navigation System for Landing</b>	Ref : <b>OPTICAL.ASTR.TN.003.09</b> Issue : 1      Rev. : 0 Date : 16/03/2009 Page : 19
---	---	--

The navigation core is mainly composed of the hybrid navigation filter. The IMU bus carries the inertial measurements at high frequency. The sensor bus brings the optical flow chain measurements at low frequency:

- ✓ The translation direction measurement, coming from the OF & egomotion function,
- ✓ The relative position to the ground at the second frame, coming from the DEM matching function,
- ✓ The raw optical flow, coming from the OF & egomotion function. This raw optical flow could be used in the navigation filter in case a homographic approach needs to be implemented. If the DEM matching function is not working for any reason, this implementation could be useful to have an additional measurement (the ratio between the velocity and the distance to the ground).

The OF & Egomotion function is divided in 2 blocks:

- ✓ The OF computation function: first the optical correlator uses two images separated by 4 frames to evaluate the maximal length of the correlation vectors. By extrapolation the optimal time interval between the two images is determined. This time interval ensures that the  $\Delta P/d$  ratio is optimal (maximizing of the signal to noise ratio and minimizing of distortion impact). Then the optical flow is computed for the two selected images, without any navigation aiding. The time interval is provided to the IMU pre-processing function to compute the delta position and attitude between the two frames. This aiding is required for the Egomotion determination.
- ✓ The egomotion function: using the raw optical flow and the attitude change between the two frames (through IMU aidings), this function computes the translation direction measurement which is part of the sensor bus provided to the navigation core. The local distances (range measurement for each elementary facet of the image) is also computed and provided to the DEM matching function. Local distances are scaled using the delta position provided by the IMU aiding.

The DEM generation function uses the different aidings (estimated position and attitude from navigation filter, delta position and attitude from IMU) and the local distances computed by the egomotion function to generate the OF-derived DEM.

This OF-derived DEM is then matched with the reference one. This matching results in a measurement of the estimation error of the relative position to the ground at the second frame. The updated relative position is then provided to the navigation filter. The operation can be repeated in an iterative process to improve the accuracy of the measurement.

## 5 NAVIGATION PERFORMANCES

The performances and sensitivity simulation campaigns have been completed by TUD in open loop in order to analyse in detail the behaviour of the navigation chain. The objective of closed loop tests performed by Astrium was to integrate the new navigation chain in a complete GNC simulator. Considering the simulation time due to the necessity to run the PANGU tool in the loop (which is not required in open loop) and to the image processing algorithms, the closed loop test plan is deliberately slight, only aiming at proving the correct integration of the optical flow based navigation function in the GNC simulator. The objective is also to give some preliminary performances of the end-to-end GNC chain that would require a dedicated Monte Carlo campaign to be consolidated.

The closed loop simulator has been integrated by Astrium using the open loop simulator and building blocks from past vision-based navigation simulators (VBNAT for NPAL, LFES for LiGNC).

### 5.1 OPEN LOOP TESTS

#### 5.1.1 Test plan

The goals of the open loop tests are the following:

1. Determination of the navigation errors dependence on the sampling rate
2. Determination of the navigation errors dependence on the trajectory location with typical initial estimation errors and optimal sampling rate
3. Evaluation of the initial estimation errors effect on the filter convergence stability
4. Analysis of the navigation errors dependence on the IMU class

The following table synthesises the general test conditions.

	Moon scenario	Mars scenario
Planetary gravitational constant	$4.89 \cdot 10^{12} \text{ m}^3/\text{s}^2$	$4.2811 \cdot 10^{13} \text{ m}^3/\text{s}^2$
Gravitational acceleration at surface	$1.62 \text{ m}/\text{s}^2$	$3.698 \text{ m}/\text{s}^2$
Planet radius	17370000 m	3402200 m
Simulation duration	47s	70s
Camera tilt around BF y-axis	$-10^\circ$	0
Camera field of view	$70^\circ$	
Camera image size	1024x1024	
Camera frame rate	5Hz	

Camera model	applied to 1024x1024 PANGU images	
Gyro scale factor	10 <sup>-5</sup> each axis	
Gyro bias	0.01°/h each axis	
Gyro noise	0.0025°/h <sup>1/2</sup> each axis	
Accelerometer scale factor	8·10 <sup>-5</sup> each axis	
Accelerometer bias	4.905·10 <sup>-4</sup> m/s each axis	
Accelerometer noise	1.4715·10 <sup>-4</sup> m/(sh <sup>1/2</sup> )	
Optical Correlator	Simplified model	
Sensors sample time	Adaptive, ≥ 1s	2s
Egomotion sensor standard deviation	1.73·10 <sup>-5</sup> along line of sight, 1.73·10 <sup>-3</sup> other axes	n/a
Position sensor bias standard deviation	20m each axis	5m each axis
Position sensor standard deviation	40m each axis	Alt. ≤ 2km: 4m each axis Alt. = 4km: 8m each axis Alt. ≥ 6km: 15m each axis
Initial position error standard deviation	192m each axis	
Initial velocity error standard deviation	3.33m/s each axis	4m/s vertical axis 10m/s horizontal axes
Initial attitude error standard deviation	0.667° each axis	

**Table 5-1 : General test conditions**

The reference DEM that has been used has a resolution of 3m. According to sensitivity tests that have been conducted, the system is practically not sensitive to reference DEM horizontal resolution until it reaches 10% of the altitude. It means, for example, that the reference DEM resolution should be better than 10m if the visual navigation phase ends at the height of 100m over the planet surface. Enlarging of

the horizontal sampling distance above 10% of altitude results in fast degradation of the DEMs matching accuracy, caused mainly by reference DEM texture becoming insufficient for correlation-based matching.

### 5.1.2 Test results (OF navigation solution / Moon Mission)

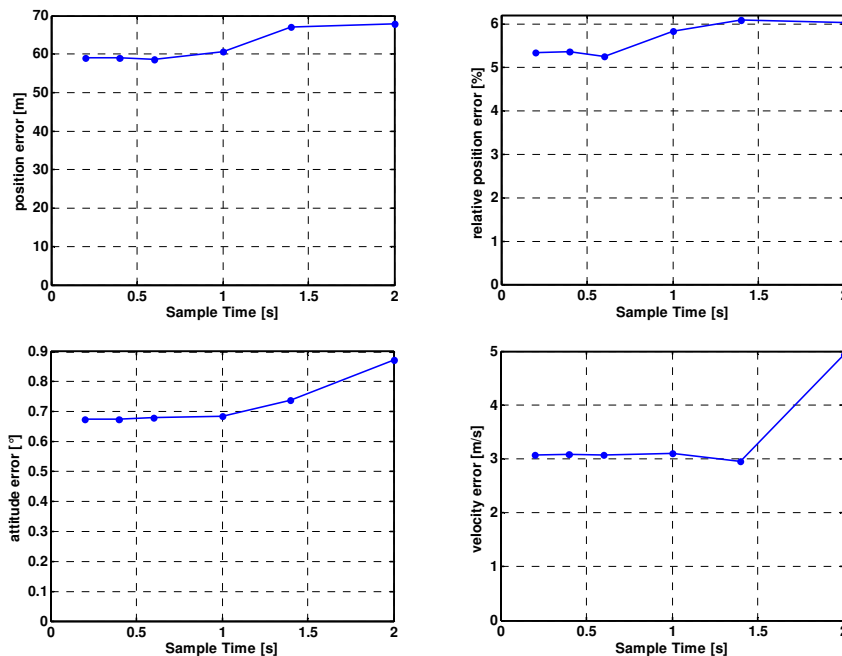
#### Navigation errors dependence on the minimal sampling rate

For this test following initial estimation errors have been applied:

- position error: 3D vector with random direction and random norm ( $\sigma = 0.33$  km);
- velocity error: random value with  $\sigma = 3.33$  m/s on each of 3 axes;
- attitude error: random value with  $\sigma = 0.66^\circ$  on each of 3 axes.

4 test flights have been performed with the same surface model; the results have been combined to reduce the dependence on the local surface properties variations. For each flight the approach direction has been changed by  $90^\circ$ . Landing points were symmetrically positioned at the distance of 500 m from the centre of the model.

The sampling interval for optical flow determination has been generally selected adaptively by the Optical Correlator Module. To investigate the effect of sampling frequency limitations, in this test the minimal sampling interval has been limited by 0.2, 0.4, 0.6, 1.0, 1.4 and 2.0s. Figure 5-1 shows the dependencies of the obtained navigation errors on the minimal sampling interval limit (to improve the statistics, navigation errors have been averaged for the time interval of 5 ... 30s of mission time).



**Figure 5-1 : Navigation errors dependency on the minimal sampling time limit (averaged for 5 ... 30 s mission time).**

On the base of the test results, minimal sampling interval limit of 1.0 s has been selected. This value has been considered for all other tests with Moon reference mission.

### Initial estimation errors effect on the convergence stability

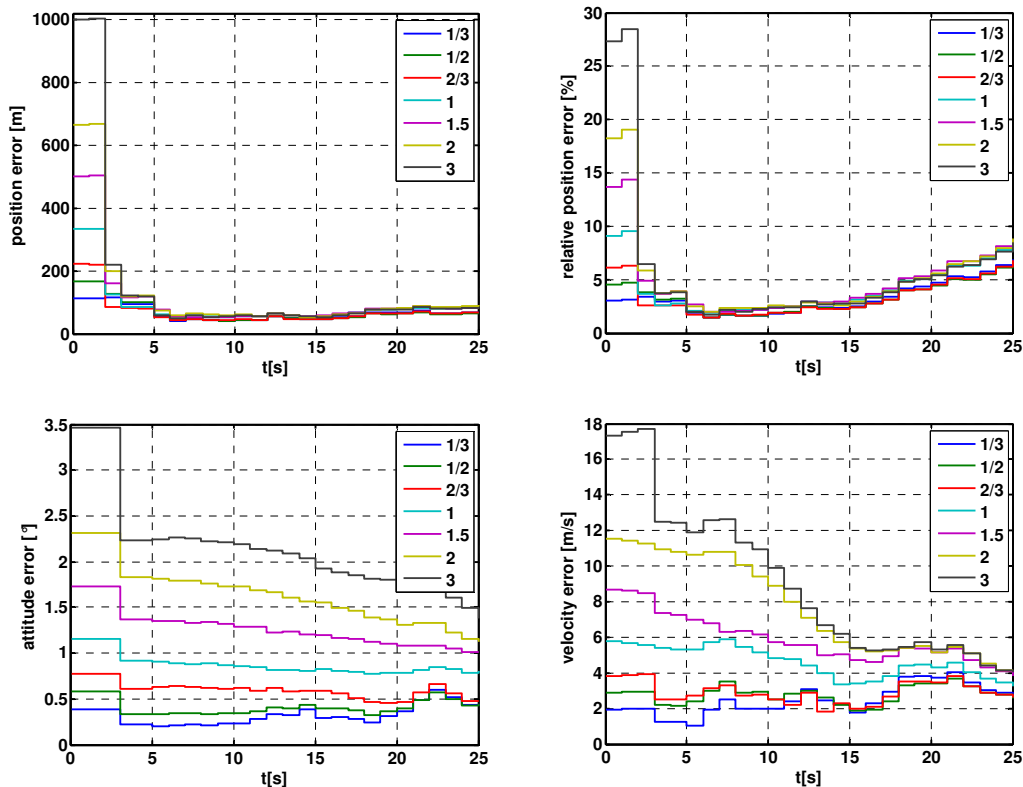
For this test the following initial estimation errors

- position error: 3D vector with random direction and norm = 0.33 km;
- velocity error: 3.33 m/s on each of 3 axes, random sign;
- attitude error:  $0.66^\circ$  on each of 3 axes, random sign;

have been multiplied by scaling coefficient  $k = 1/3; 1/2; 2/3; 1; 1.5; 2; 3$ . For initial errors with scaling coefficient  $k = 3$  ( $3\sigma$ ) initial filter standard deviations have been multiplied by 1.5 to avoid inconsistent innovations during measurement update.

4 test flights have been performed with the same surface model; the results have been combined to reduce the dependence on the local surface properties variations. For each flight the approach direction has been changed by  $90^\circ$ . Landing points were symmetrically positioned at the distance of 500 m from the centre of the model.

The sampling interval for optical flow determination has been selected adaptively by the Optical Correlator Module; minimal sampling interval value has been limited at 1.0 s. Figure 5-2 shows the navigation errors (RSS for 3 axes) obtained with different scaling coefficient values.



**Figure 5-2 : Navigation errors (RSS for 3 axes) obtained with different values of initial estimation errors scaling coefficient**

As a result of the test, stable convergence has been observed with position error of up to 1000 m (27% of the altitude), attitude error of up to 3.42 degrees and velocity error of up to 17.3 m/s.

### 5.1.3 Test Results (VOF Navigation solution / Mars Mission)

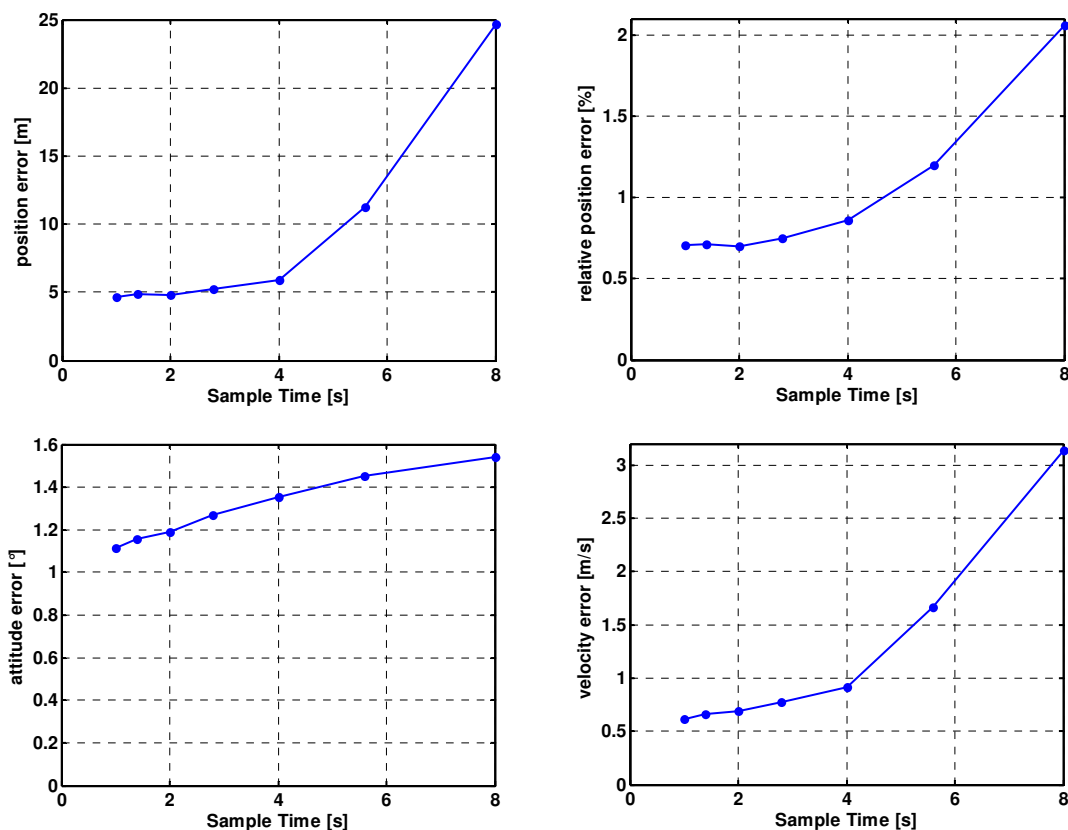
#### Navigation errors dependence on the minimal sampling rate

For this test following initial estimation errors have been applied:

- position error: 3D vector with random direction and random norm ( $\sigma = 0.33$  km);
- velocity error: random value with  $\sigma = 10$  m/s on each of 2 horizontal axes;
- velocity error: random value with  $\sigma = 4$  m/s on the vertical axis;
- attitude error: random value with  $\sigma = 0.66^\circ$  on each of 3 axes.

4 test flights have been performed with the same surface model; the results have been combined to reduce the dependence on the local surface properties variations. For each flight the approach direction has been changed by  $90^\circ$ . Landing points were symmetrically positioned at the distance of 500 m from the centre of the model.

To investigate the effect of sampling frequency limitations, the test has been performed with the sampling interval values 1.0, 1.4, 2.0, 2.8, 4.0, 5.6 and 8.0 seconds. Figure 5-3 shows the obtained navigation errors dependencies on the sampling interval value (to improve the statistics, navigation errors have been averaged for the time interval of 20 ... 60s of mission time).



**Figure 5-3 : Navigation errors dependencies on the sampling interval value.**

On the base of the test results, sampling interval value of 2.0 s has been selected. This value has been considered for all other tests with Mars reference mission.



### Initial estimation errors effect on the convergence stability

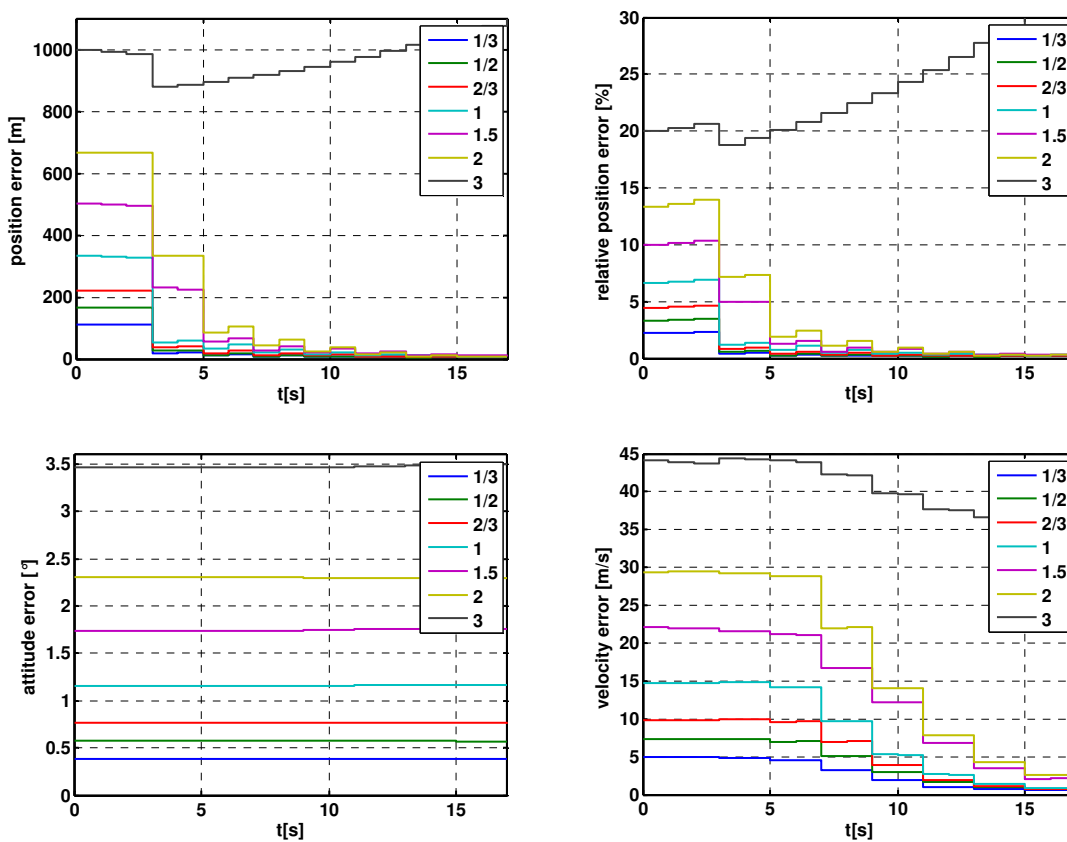
For this test the following initial estimation errors

- position error: 3D vector with random direction and norm = 0.33 km;
- velocity error: 10 m/s on each of 2 horizontal axes, random sign;
- velocity error: 4 m/s on the vertical axis, random sign;
- attitude error:  $0.66^\circ$  on each of 3 axes, random sign.

have been multiplied by scaling coefficient  $k = 1/3; 1/2; 2/3; 1; 1.5; 2; 3$ . For initial errors with scaling coefficient  $k = 3$  ( $3\sigma$ ) initial filter standard deviations have been multiplied by 1.5 to avoid inconsistent innovations during measurement update.

4 test flights have been performed with the same surface model; the results have been combined to reduce the dependence on the local surface properties variations. For each flight the approach direction has been changed by  $90^\circ$ . Landing points were symmetrically positioned at the distance of 500 m from the centre of the model.

The test has been performed with sampling interval 2.0 seconds. Figure 5-4 shows the navigation errors (RSS for 3 axes) obtained with different scaling coefficient values.



**Figure 5-4 : Navigation errors (RSS for 3 axes) obtained with different values of initial estimation errors scaling coefficient**

As a result of the test, stable convergence has been observed with position error of up to 670 m (13.4% of the altitude) and velocity error of up to 29 m/s. Attitude convergence is very slow (for the vertical axis no convergence is possible at all because it is not observable with the current configuration (position sensor only)). The VOF navigation principle however allows precise absolute attitude determination - this possibility just has not been used in this test configuration and has not been considered in the navigation filter.

#### **5.1.4 Conclusion of the open loop tests**

The open loop tests have proved the good stability of the navigation chain and its robustness to a large range of initial navigation errors (1000m and 17m/s for Moon, 500m and 30m/s for Mars). Attitude convergence is very slow since the possibility of estimating the attitude through optical flow measurements has not been used on purpose in order to ensure the robustness of the navigation chain and avoid loops between the navigation filter and optical flow algorithms. This possibility could however be analysed as an improvement of the navigation chain.

The open loop tests have also shown some issues with PANGU when rendering images: the lack of high spatial frequency texture in the late images of the sequence has a significant impact on the navigation performances. Therefore the final performances obtained during the open loop tests can be considered as worst case and would have been better with realistic images. Such realistic images can be obtained for the low altitude either with a better parameterization of PANGU, or with an upgrade of PANGU.

## **5.2 CLOSED LOOP TESTS**

### **5.2.1 Simulator integration**

The closed loop simulator has been integrated using the open loop building blocks (sensors and navigation function), and elements from 2 existing vision-based navigation simulators:

- LFES (Landing Functional Engineering Simulator) is the simulator developed in the LiGNC study. A strong effort has been made to integrate the Guidance & Control function coming from LiGNC in the optical flow simulator. The actuators block as well as the dynamics block has also been reused.
- VBNAT (Vision-Based Navigation Analysis Tool) is the NPAL simulator. The camera model has been adapted from VBNAT for optical flow, and the dynamics under parachute has been reused for the Mars scenario (it is not modelled in the LiGNC study).

### 5.2.2 Objectives of the closed loop simulations and test plan

The major objective of the closed loop simulations is to prove the correct integration of the optical flow based navigation function in the GNC simulator, and to give some preliminary performances of the end-to-end GNC chain. These preliminary results would require a dedicated Monte Carlo campaign to be consolidated.

Considering the high simulation time due to the necessity to have PANGU in the loop and the computation time of image processing algorithms, a single simulation has been run for both Mars and Moon scenario. The same test conditions have been applied as for the open loop tests (see Table 5-1). The initial navigation errors have been set considering the convergence domain established by the open loop tests. Weak attitude errors have been applied considering the slow attitude convergence in the selected navigation architecture.

The following table indicates the initial navigation errors that have been considered. Values are given in the LDS frame (linked to the terrain, Z axis is vertical).

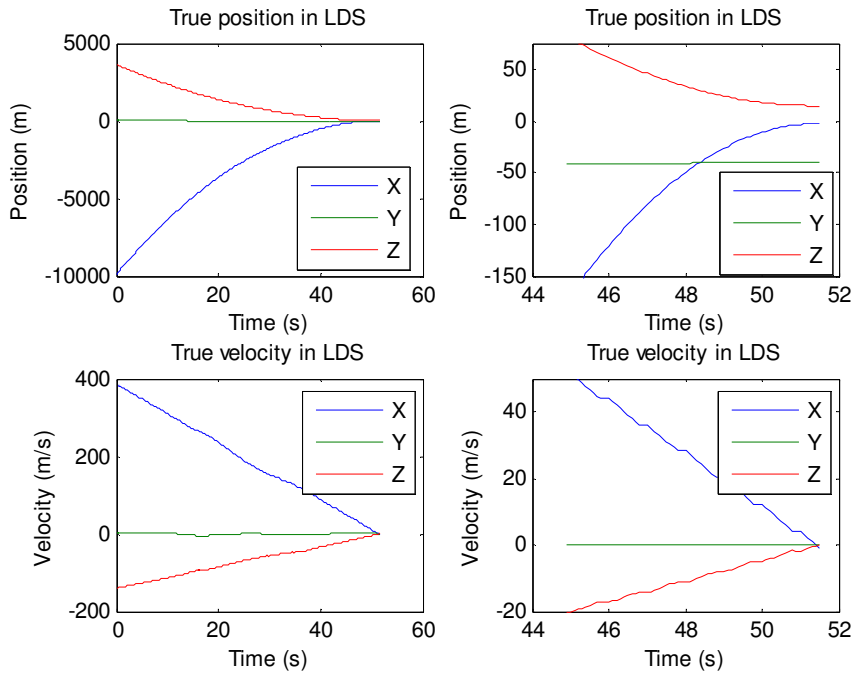
	Mars Scenario	Moon Scenario
<b>Initial position error (m)</b>	[330;330;330]	[1000;1000;1000]
<b>Initial velocity error (m)</b>	[10;10;4]	[10;10;10]
<b>Initial attitude error (deg)</b>	[0.2;0.2;0.2]	[0.1;0.1;0.1]

**Table 5-2 : Initial navigation errors for the closed loop simulations**

### 5.2.3 Tests results

#### Moon scenario

Figure 5-5 plots the true position and velocity in the LDS frame. One can check that the spacecraft safely lands on the surface. The control accuracy at touchdown is better than 1 m/s in velocity and 40m in position. This validates the good behaviour of the GNC closed loop.

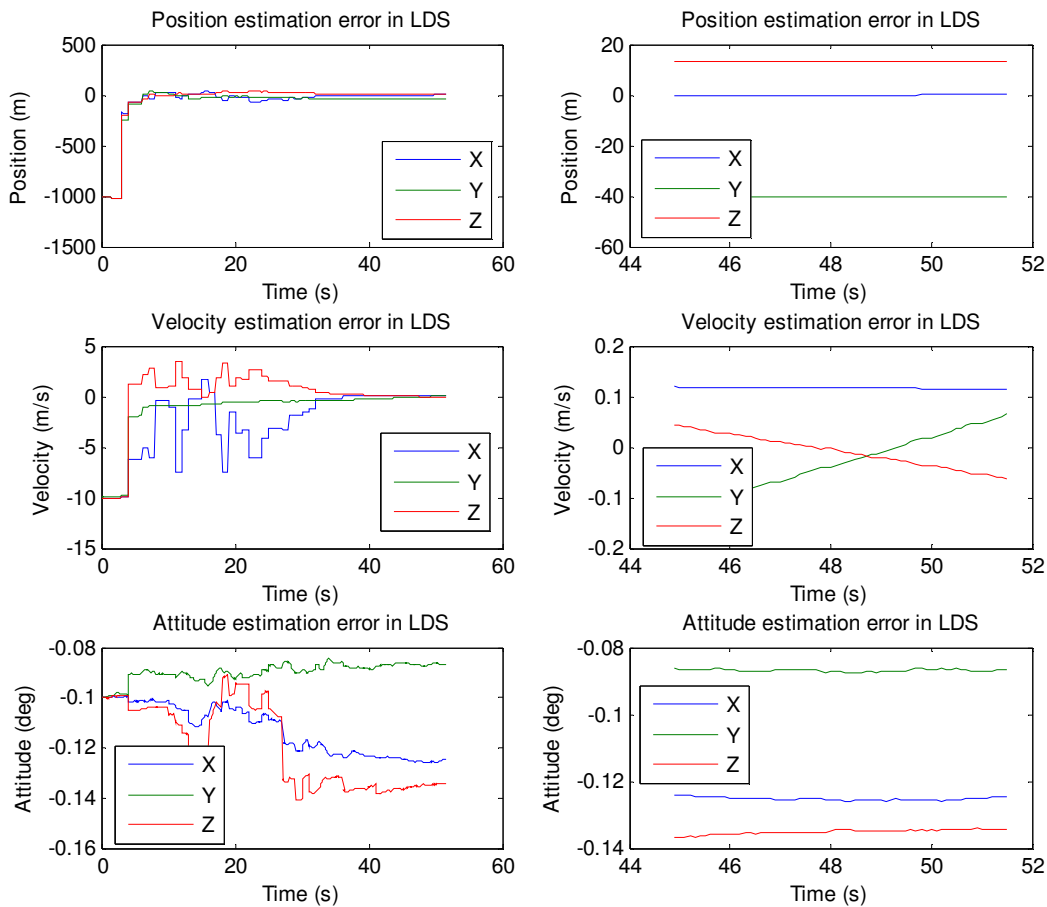


**Figure 5-5 : Moon scenario - True position and velocity in LDS**

Figure 5-6 shows the navigation errors during the descent. One can see that the position measurement coming from DEM generation and matching allows a fast convergence of the position. The final performance of the position estimation impacts directly the control accuracy, as one can see on Figure 5-5.

The Egomotion function is a little slower to converge but the final performance of the velocity estimation is quite good (about 0.1 m/s).

The weak attitude error is almost not observable considering the architecture choice that has been made for this study.

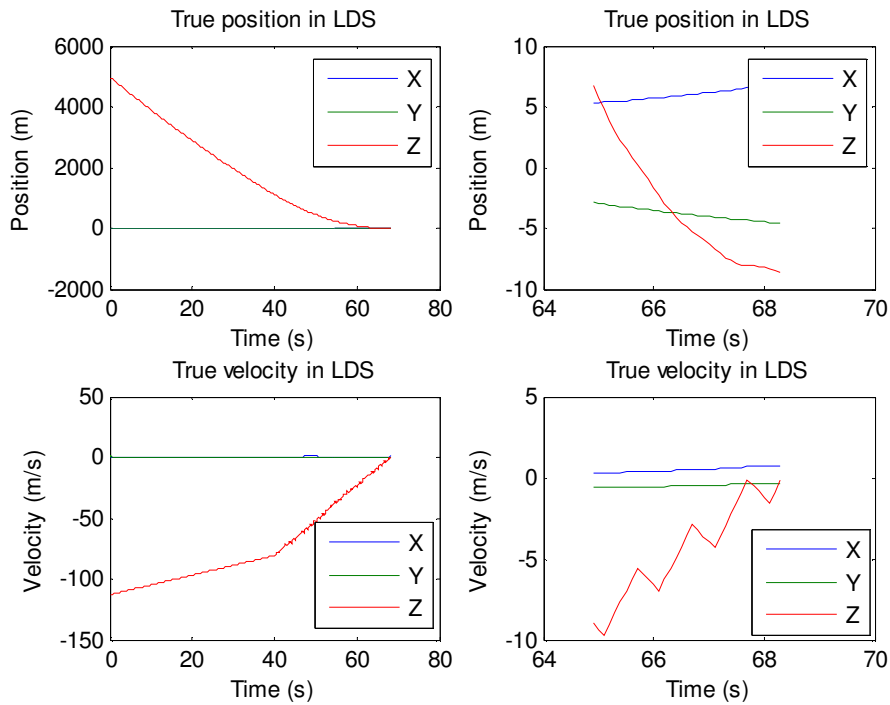


**Figure 5-6 : Moon scenario - Estimation errors**

These results show that the navigation chain is well integrated in the GNC simulator, and that the system is stable and good performing. A safe and precise landing is ensured and the navigation function convergence is good. However the guidance function shows a lack of robustness that can be an issue when large initial navigation errors are considered (if thrusters are saturated during a long time, then the spacecraft is not able to follow the reference trajectory and the landing is not safe). This guidance function shall therefore be improved for the specific needs of optical flow scenarios.

### Mars scenario

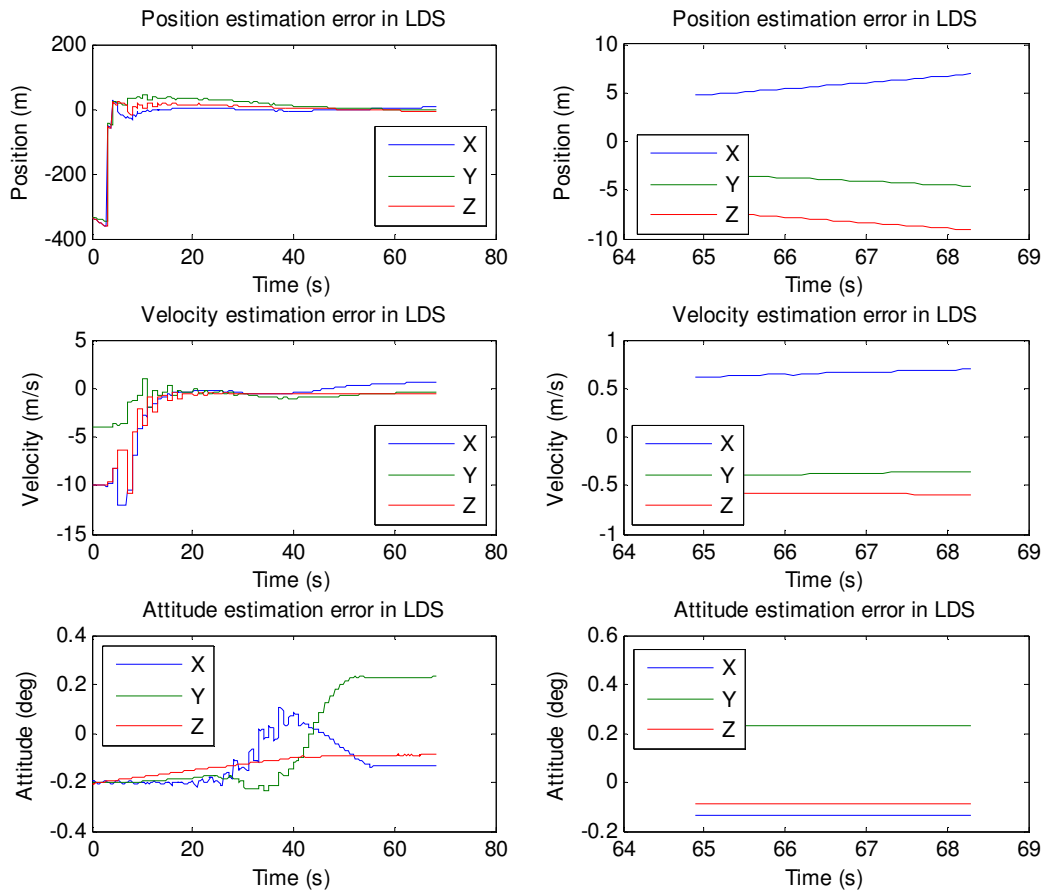
Figure 5-7 plots the true state in LDS (terrain frame, Z is vertical) for the Mars scenario. The first 40 seconds are not controlled: the spacecraft is under the parachute and the guidance and control function is disabled. Thrusters are not actuated. At t=40 the parachute is jettisoned and the control is activated. The control accuracy at touchdown is quite good: a few meters in position, a few 0.1 cm/s in velocity.



**Figure 5-7 : Mars scenario – true position and velocity in LDS**

Figure 5-8 plots the estimation errors during the descent. The VOF solution allows a fast and very accurate convergence of the position estimation, with a final performance better than 10m thus allowing a precise landing. The velocity convergence is ensured in less than 20 seconds. This means that the estimated state is quite accurate when the parachute is jettisoned and the control is activated at  $t=40s$ .

The weak attitude error is almost not observable considering the architecture choice that has been made for this study.




**Figure 5-8 : Mars scenario – Estimation errors**

The results show that the closed loop is stable and good performing for the Mars scenario.

#### 5.2.4 Conclusions of the closed loop tests

The closed loop simulations have shown that the optical flow based navigation function is now well integrated in the complete simulator. The full GNC chain is stable and shows quite good performances. The optical flow solution allows a safe and precise landing. These promising preliminary results should be consolidated with a dedicated closed loop Monte Carlo campaign.

The guidance function should be improved in robustness for the specific needs of optical flow scenarios in order to be able to cope with large initial navigation errors. The simulations show that the MBTL is not always able to define a reference trajectory without saturating the thrusters in this case, which is not a safe situation. It is proposed to optimise the time to go parameter instead of having a constant parameter in order to resolve this problem.

	<b>Optical Flow Navigation System for Landing</b>	Ref : <b>OPTICAL.ASTR.TN.003.09</b> Issue : 1      Rev. : 0 Date : 16/03/2009 Page : 32
---	---	--

## 6 CONCLUSION AND PERSPECTIVES

### 6.1 AN INNOVATIVE VISION-BASED NAVIGATION TECHNOLOGY FOR LANDING

In the continuation of the past two studies jointly led by Astrium and TUD, the OFNSL study has successfully reached its objectives:


- The specificity of optical flow measurements has been understood and a comprehensive navigation chain has been built upon the assets of the technology, with a dedicate adaptation of the navigation filter to ensure the robustness and the stability of the concept.
- The navigation design has been validated through an intensive open-loop simulation campaign, that underlined the good performances of both OF and VOF solution for the selected reference scenarios.
- This brand new navigation chain has been successfully integrated in a complete GNC chain using the results of past vision-based navigation studies for the guidance & control function. The results of the preliminary closed loop simulations show that interfacing issues between the navigation function and the guidance & control function have been mastered. Preliminary performances are very promising: the GNC chain allows a safe and precise landing.

The performances simulations have pointed out that the lack of high spatial frequencies in PANGU images at the end of the sequence has an impact on navigation performances. In realistic images it is believed that fractal behaviour would lead to performances similar to the ones observed at the beginning of the sequence. This simulation issue should be solved (either with a different parameterization of PANGU, or with an upgrade of the tool) to analyse precisely the navigation performances at touchdown. In the context of the study, the navigation performances can be considered as worst case figures.

Compared to navigation specifications, it appears that the 10m specification in position estimation at touchdown is not met. As stated before, this conclusion is to be mitigated by the impact of the lack of high spatial frequencies in images at the end of the trajectory. However the position estimation performance is about a few tens of meters, with a very fast convergence, thus allowing an early and good positioning of the spacecraft in a frame related to the target. The major innovation of the concept is that this positioning is absolute, using a reference terrain model on board the flight software. This is of high interest when the spacecraft shall land at a pre-defined landing site, as it is the case for scientific missions with high environment constraints (for example, landing at the Peak of eternal light on the Moon, or in a specific crater of Mars), or when the landing site designation can be made during in-orbit characterization of the target (as it is the case for the Marco Polo mission).

However relative navigation techniques are really good solutions to avoid the detected hazards just before the touchdown, and to increase the robustness of the system in case of high initial dispersion of the lander's state (relative navigation techniques do not need a reference terrain model and can operate in unknown environment).



	<b>Optical Flow Navigation System for Landing</b>	Ref : <b>OPTICAL.ASTR.TN.003.09</b> Issue : 1      Rev. : 0 Date : 16/03/2009 Page : 33
---	---	--

It is therefore believed that optical flow techniques associated with relative navigation solution (such as NPAL) would ensure a safe, robust, autonomous and accurate landing on any target. This association would need to be analysed in a dedicated study.

A key point in this technology is the reference terrain model. Navigation performances strongly depend on the resolution of this reference DEM. The different possibilities to get this accurate reference terrain model on orbit would need to be further investigated in order to secure this major phase of the mission.

During this study the priority has been given to the robustness and the stability of the navigation chain. This goal has been successfully reached but it results in a poor observability of the attitude relatively to the terrain that needs to be controlled in order to ensure a safe landing. This could be solved using additional sensor, or with an upgrade of the navigation chain: OF and VOF techniques both allow the determination of the attitude of the spacecraft in the position determination function. This possibility has been just disabled in this study to avoid as much as possible loops between image processing algorithms and the navigation filter that can endanger the stability of the loop. On the base of the navigation chain developed in this study, this specific point could be further addressed and optimised to get the observability of the relative attitude to the terrain.

## 6.2 PRELIMINARY DEVELOPMENT PLAN FOR A FLIGHT EXPERIMENT

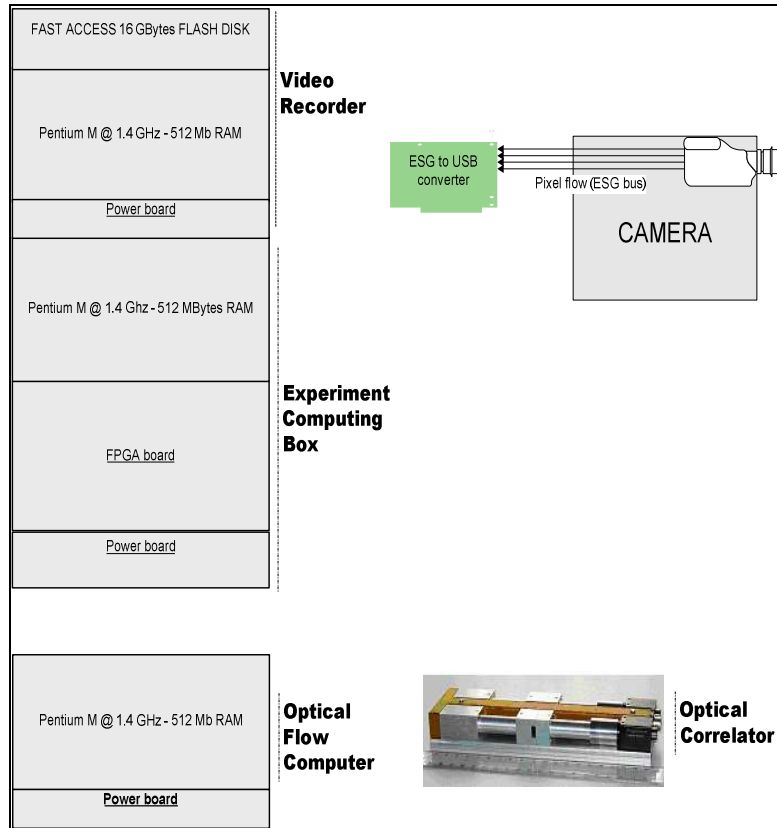
A preliminary assessment of the main constraints to make a flight experiment of the optical flow navigation chain on board the PLGTF has been performed.

The PLGTF setup needs to be extended to support the new functions brought by optical flow experiment. These new elements, the optical correlator and its associated computing unit, must also be able to fly within the embedded harsh environment of PLGTF helicopter, with limited mass and power budgets.

To reduce technical risks and engineering costs (i.e. design effort and procurement), we propose the following solution: a new PC104+ computer is dedicated to optical flow function: the **Optical Flow Computer (OFC)**

- OFC is made of the same commercial boards (CPU & power) as the video recorder and ECB ones.
- OFC is mounted as a separate PC104+ stack, mechanically and electrically independent of ECB & VREC stack.
- The onboard Ethernet network is the only functional interface of the OFC

The whole configuration (in terms of equipment) PLGTF + Optical flow becomes:



**Figure 6-1 : PLGTF and OPTICAL FLOW equipment**

The following important points have still to be addressed:

- Optical correlator ruggedization (with regard to vibrations / dust / thermal / power issues)
- Interface HW between the optical correlator and the computer (OFC)
- SW interface with PLGTF
  - Images: acquisition frequency, size , format...
- Processing power:

It is supposed here that the CPU is powerful enough to enable the complete processing by SW.

This should be confirmed by a “benchmarking campaign” of the algorithms.

Nevertheless, if the “full SW” solution was not possible, an extra PC104+ FPGA board could be accommodated into the OFC stack. The part of image processing that could be then implemented in VHDL is to be defined.

**DISTRIBUTION LIST**

	Overall document		Summary
	Action	Information	
<b>Astrium Satellites SAS</b>			
G. FLANDIN	X		
B. POLLE	X		
C. CAVEL	X		
J. MORAND		X	
GED			
<b>TUD</b>			
K. JANSCHKE	X		
<b>ESA</b>			
L. LOPES	X		
C. PHILIPPE	X		